15415 FERROAN ANORTHOSITE ST. 7 269.4 g

INTRODUCTION: 15415 ("Genesis Rock") consists almost entirely of anorthite, and is a coarse-grained, ferroan crystalline rock with a complex cataclastic and metamorphic history. It was originally a plagioclase cumulate from a liquid with a near-chondritic rare earth pattern and rare earth abundances perhaps 10x chondrites. The source of the 15415 parent liquid was separated from a chondritic Rb/Sr reservoir very early in lunar history. Ar-Ar ages of ~4.0 b.y. probably represent later heating events, not original igneous crystallization.

15415 is a pale, blocky, angular to subrounded sample, which was originally partly dust-covered (Fig. 1). Some individual pieces are tough, but penetration fracturing makes some portions friable. The surface was hackly on fresh faces; zap pits were present on only one (S) surface. 15415 was collected from the northern lip of Spur Crater, where it was perched on a clump which was sampled as 15435 to 15437. It is generally believed (e.g., Wilshire et al., 1972) that 15415 was a clast in a friable soil breccia or clod represented by the clump. It rested on a gentle slope of several degrees to the south towards the bottom of Spur Crater. It was especially noted by the Apollo 15 crew as "something close to anorthosite, because it's crystalline and ... just almost all plag." (Bailey and Ulrich, 1975).

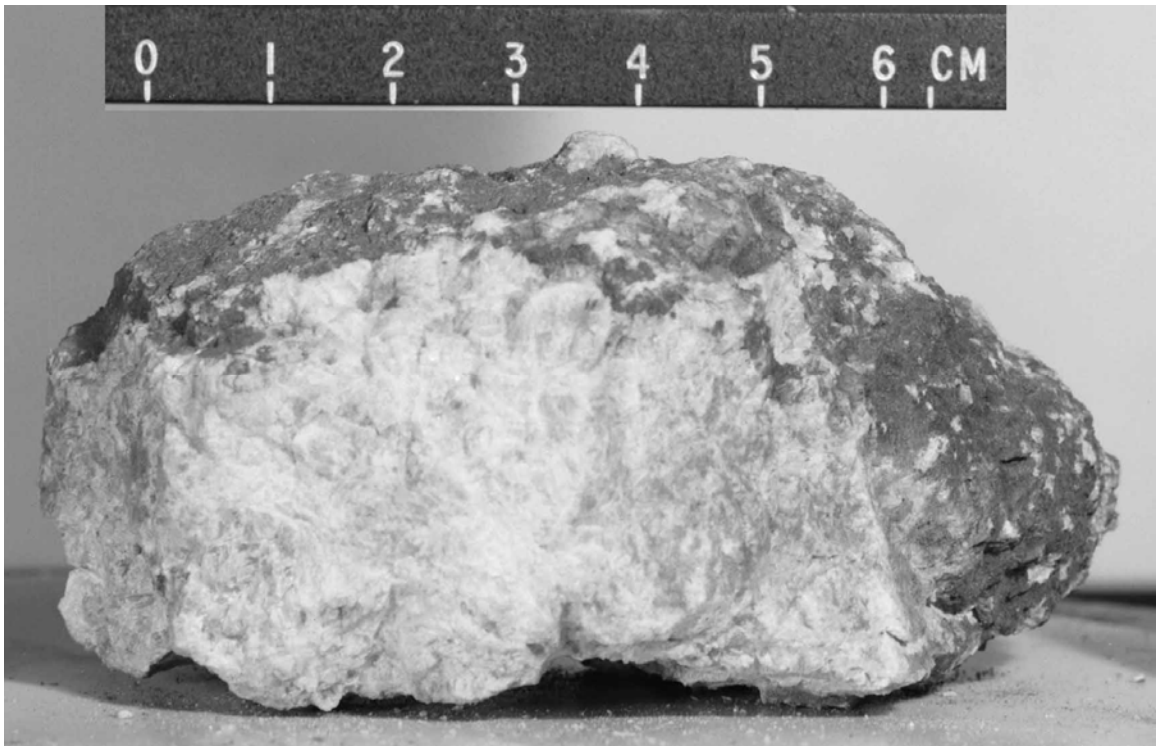

Figure 1. Pre-split view of ,0, showing white anorthosite and gray dust. S-71-44998

PETROLOGY: 15415 consists almost entirely of anorthite crystals, with minor iron-rich mafic minerals consisting mainly of diopsidic augite, and traces of hypersthene, ilmenite, and a silica mineral. The plagioclase content may be greater than 99%, but the textural heterogeneity precludes an accurate nodal determination from single subsamples. The textures (Fig. 2) demonstrate a complex cataclastic and metamorphic history, following an origin by accumulation from a plagioclase saturated magma.

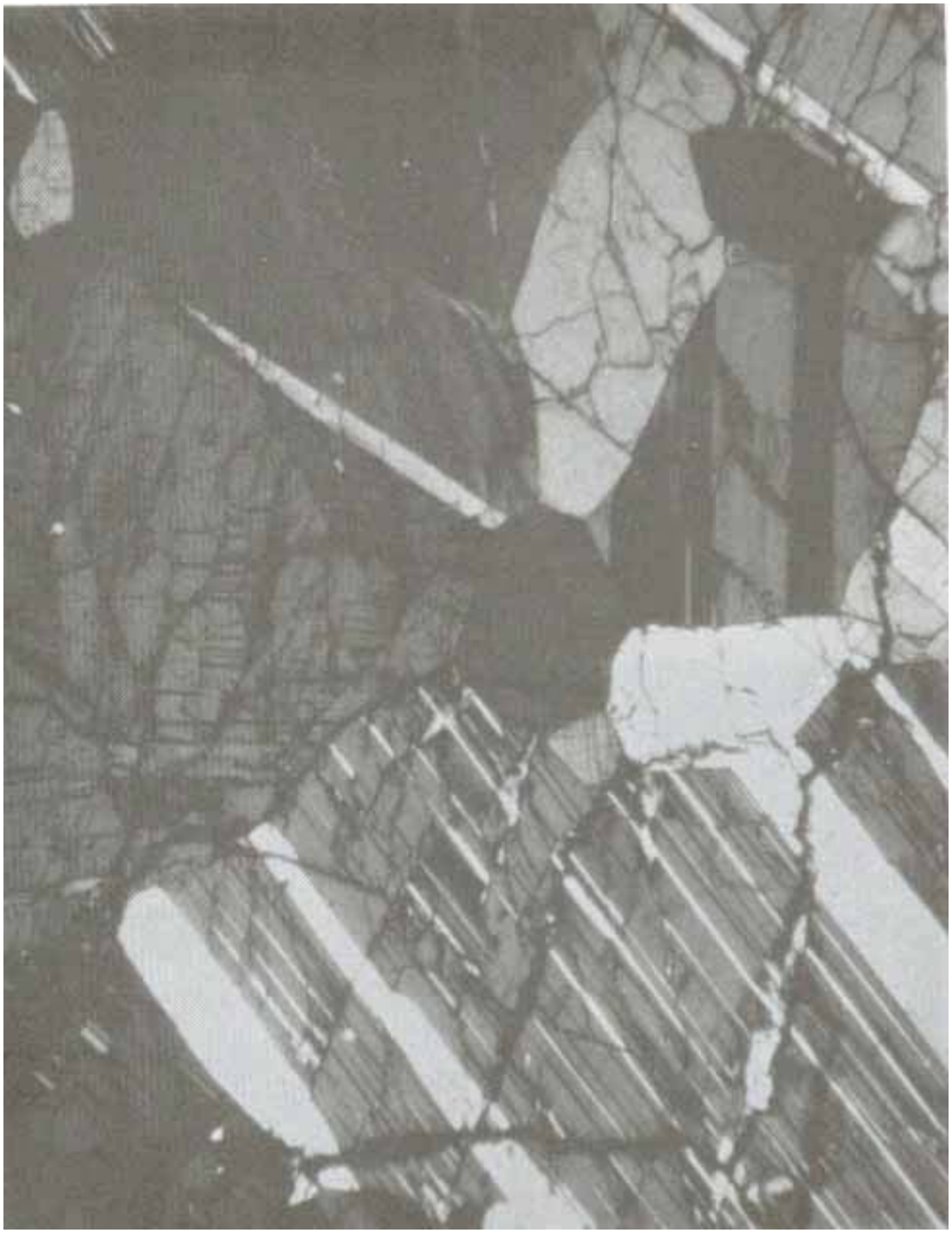

Fig. 2a

Fig. 2b

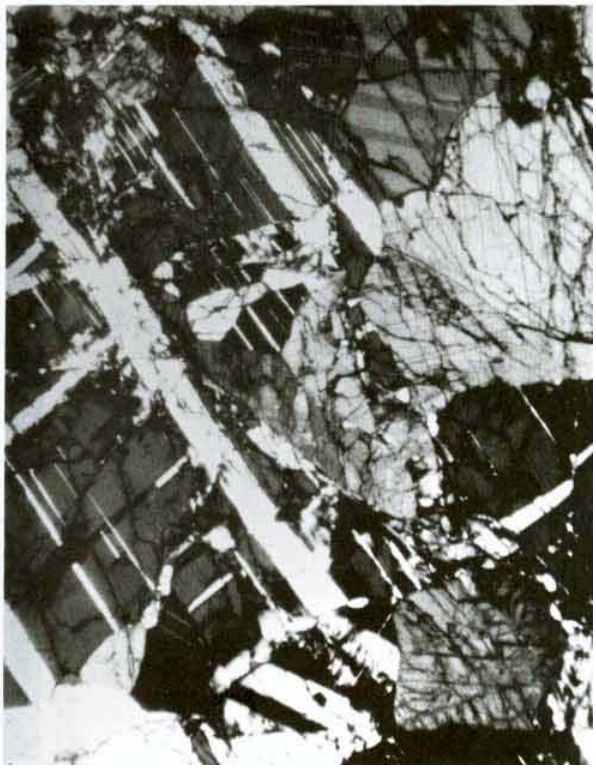

Fig. 2c

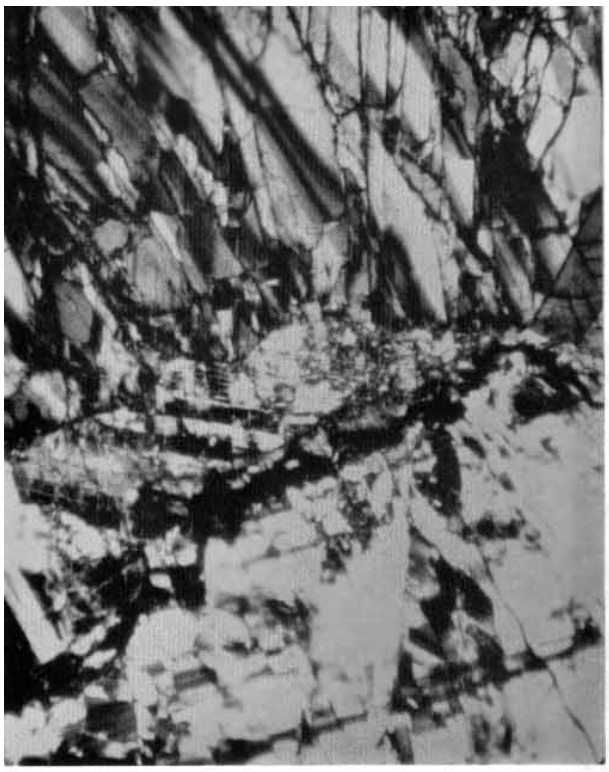

Fig. 2d

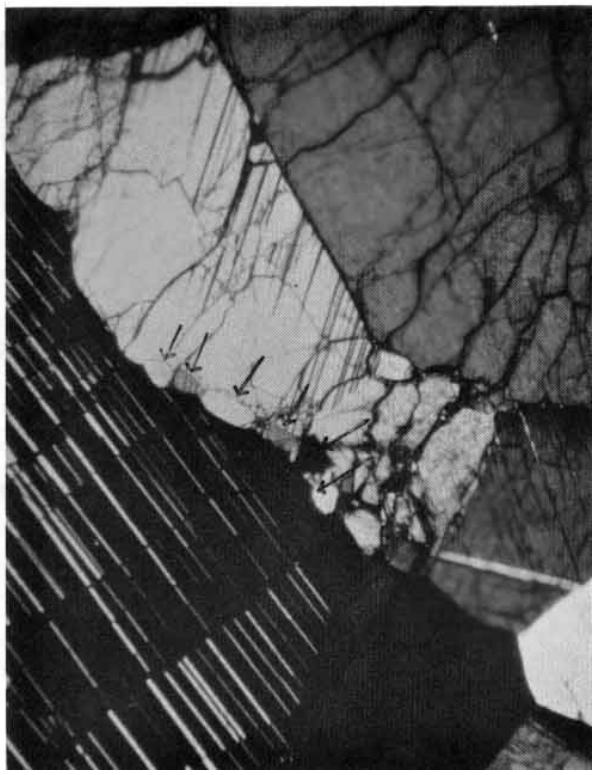

Fig. 2e

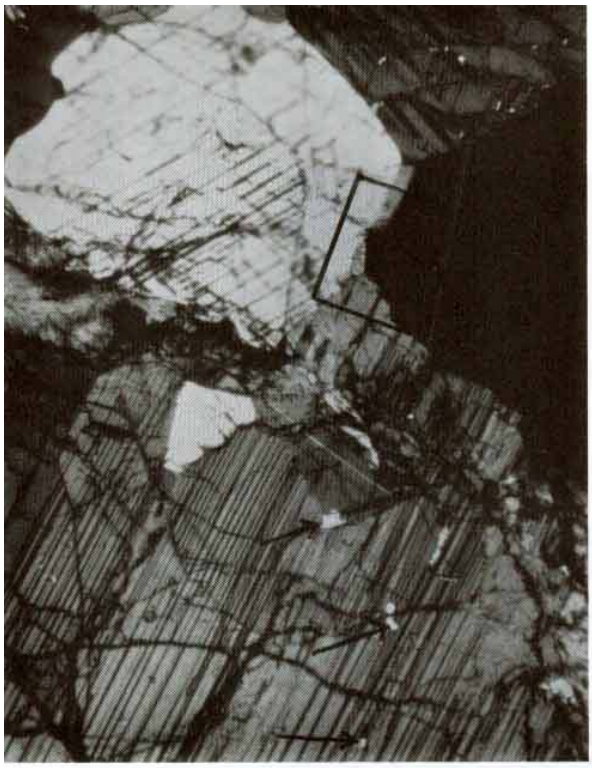

Fig. 2f

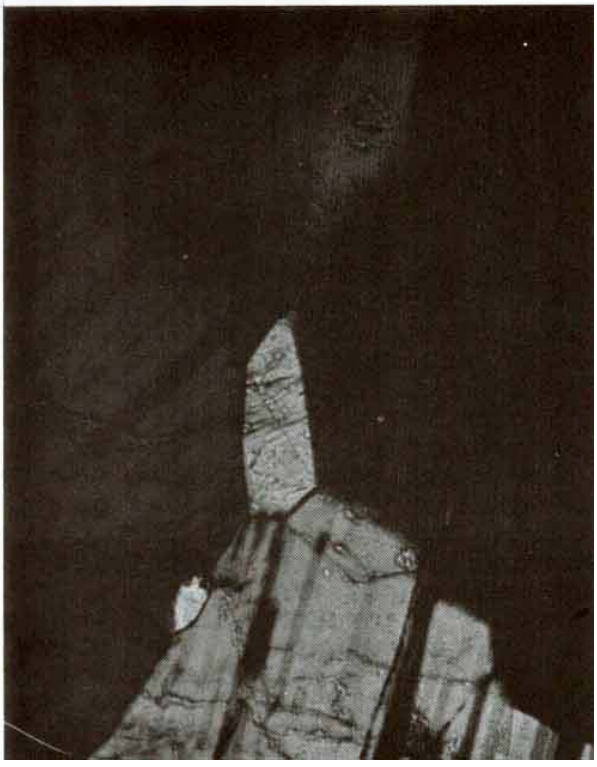

Fig. 2g

Fig. 2h

Figure 2. Photomicrographs of 15415, all crossed polarizers, all widths about 2 mm except g and h, whose widths are about 300 microns.
a) 15415,19, general view: polygonal grains with curving boundaries, fracturing, and mechanical twins.
b) 15415,15: bands of small polygonal plagioclases cutting single large plagioclase.
c) 15415,19: cataclasized, annealed region.
d) 15415,94: large shock deformed plagioclase crystals.
e) 15415,92: pyroxenes (arrows) along plagioclase grain boundaries. Large plagioclase in bottom left shows parallel fractures and mechanical twins.
f) 15415,19: large plagioclase at bottom shows inclusions of plagioclase (e.g., arrows); rectangle in top center shows augite at triple junction.
g) 15415,19: blow-up rectangle in (f) showing two augites at plagioclase grain boundaries.
h) 15415,19: pyroxene inclusions in large plagioclase.

Comprehensive descriptions and interpretations were provided by James (1972), Hargraves and Hollister (1972), Steele and Smith (1971), Wilshire et al. (1972), and Stewart et al. (1972), and are in essential agreement. Dixon and Papike (1975) included 15415 in their Group 1, the group of least-shock-damaged anorthosites. The plagioclase is highly inequigranular, with the largest grains up to 3 cm (as seen in hand specimen) and down to below resolution. In thin section, the largest grains are anhedral and form a coarse granular mosaic. Intermediate-sized grains (1.3 to 0.1 mm) form polygons with plane or smoothly curving boundaries, in patches which cut the larger grains. Both textural types are cut by pervasive shear fractures and contain abundant deformation features, including extinction variation and mechanical twinning. Both primary and deformation twinning include pericline and albite twins. Diopsidic augite forms equant inclusions in plagioclase; polygons along grain boundaries; polygons intergrown with polygonal plagioclase; and then septa between large plagioclase grains. All are tiny (less than 200 microns), and some show exsolution (both pigeonite and orthopyroxene recognized). Augite shows the same deformation features as plagioclase, but not so abundantly developed. Hargraves and Hollister (1972) found that four augite grains in their thin section had their optic planes and c-axes more or less parallel, suggestive of the grains being a single poikilitic crystal. Hypersthene forms rare discrete grains; there is no optical evidence that it crystallized as pigeonite according to Hargraves and Hollister (1972), whereas Stewart et al. (1972) specifically noted pigeonite as well as orthopyroxene. Ilmenite occurs within pyroxene grains, and the silica occurs in several modes, included in plagioclase for example. Wilshire et al.(1972) tentatively identified traces of apatite and olivine, but neither phase has been confirmed. Hewins and Goldstein (1975) found and analyzed three minute grains of Ni- and Co-free iron metal.

Microprobe data is generally consistent. The plagioclase compositions are calcic and homogeneous (Table 1), although Hargraves and Hollister (1972) used step-scanning to find a slight compositional variation. A single analysis (An_{96-8}) listed by Dixon and Papike (1975) is consistent with the data in Table 1. Hansen et al. (1979) also reported precise microprobe analyses for MgO (0.05 ± 0.006%), FeO (0.102 ± 0.011%), and K_2O (0.023 ± 0.005%) (uncertainties 1 sigma), averages for 30 analyses of plagioclase. Ion microprobe analyses for several trace elements are listed in Table 2. The data are fairly consistent with each other and with other analyses (e.g., isotope dilution for plagiophile elements, microprobe for K, Mg). Palme et al. (1984) reported INAA analyses for five plagioclase separates (Table 3), showing the low abundances of rare earths and transition metals. Schurmann and Hafner (1972) performed Mossbauer analysis on carefully handpicked plagioclases, finding two distinct Fe^{2+} peaks, with a spectra indistinguishable from lunar basalt plagioclases. The data indicate a rapid crystallization and cooling event at some time later than the plutonic crystallization; heating to 1000°C for two days produced no change. They determined $Fe^{3+}/(Fe^{2+} + Fe^{3+})$ to be 0.04. Niebuhr et al. (1973) used electron spin resonance on three millimeter-sized anorthite single crystals to confirm that about 1% of the iron is ferric (in the tetrahedrally coordinated Al^{3+} position).

Lally et al. (1972), Heuer et al. (1972a,b), and Nord et al. (1973) reported and discussed HVEM crystallographic data. Plagioclase grains showed undeformed albite and pericline twins, and all contain 1 to 2% augite inclusions. A thin section showed fracture and deformation of twins; many regions were free of deformation, but others showed deformation and recovery (dense arrays of dislocations, etc.). The c-type domains are

large and easily imaged. Strong "c" and "d" type diffraction spots indicated P1 symmetry; samples were heated to observe the I1 to P1 phase transition. Czank et al. (1973) made precession photographs of the (b*c*) reciprocal lattice plane in plagioclase. Strong c-reflections are consistent with a high An content and a slow cooling rate. Stewart et al. (1972) reported optical properties and powder diffraction data. They also reported single crystal x-ray and electron diffraction results, finding the space group to be P1, and the properties indicate a high degree of short and long range order.

TABLE 15415-1. An-contents of plagioclases

Reference	Average	Range
James (1972)	96.6 ± 1.2	
Hargraves and Hollister (1972)		96-98
Steele and Smith (1971)	97.6	96.7-99.0
Lally et al. (1972)		93-95
Stewart et al. (1972)	96.5	
Hansen et al. (1979)	96.1	

Pyroxene compositions were reported by James (1972), Hargraves and Hollister (1972), Steele and Smith (1971), Stewart et al. (1972), and Evans et al. (1978). Data are consistent (Fig. 3), generally about $En_{40}Wo_{45}$ for host augites, and about $En_{57}Wo_3$ for exsolved hypersthene. Stewart et al. (1972) interpreted the first crystallized pyroxene to have been augite, followed by pigeonite; both became more Fe-rich by fractional crystallization. They estimated crystallization at 1150°C for one augite, and 1030°C for a pigeonite, from comparison homogenization experiments. Evans et al. (1978) made a detailed study of the crystal structure and thermal history of a single crystal of untwinned orthopyroxene, giving crystallographic data. They found a space group Pbca, and a high degree of order expected for metamorphism at 500°C,or even lower. There was no post-metamorphic thermal event which disordered it, so the 4.05 b.y. Ar-Ar age (Turner, 1972; Husain et al., 1972) is interpreted as the age of termination of the metamorphism. Post-4.05 b.y. events, which produced only a little Ar loss, had no effect on the pyroxene ordering. Smith and Steele (1974) described the pyroxene occurrences and compositions, and found that the (Fe/Mg) augite(Fe/Mg) orthopyroxene is 0.55, like terrestrial granulites, and unlike the 0.73 or so of terrestrial igneous rocks, again suggesting meta-orphism. The Mg/Fe distribution between ilmenite and low-Ca pyroxene suggests 650°C to 800°C. Smith and Steele (1974)suggested that plagioclase exsolved pyroxene plus silica plus ilmenite, questioning the assumption of any primary pyroxene. If the pyroxene were primary, the parent magma for 15415 would have atomic Mg/(Mg+Fe) of about 0.4; if exsolved, then parental Mg/(Mg+Fe) would be about 0.8, a very significant difference.

Roedder and Weiblen (1972) reported that a large number of inclusions, most less than 1 micron across, outline the main fractures. The inclusions were too small for positive identification, but some appear to be gas (sic) (which is probably a typographic error and intended to be glass), others presumably pyroxene. Simmons et al. (1975) used 15415,91 to illustrate shock-induced cracks which are subparallel, transgranular fractures. They believed that the granulated grain boundaries were a product of cataclasis (tectonic) rather than impact.

TABLE 15415-2. Trace elements in plagioclase, ion probe analyses (ppm).

Reference	Ab %	Li	Mg	K	Ti	Sr	Ba
Meyer et al. (1974)		1.6	280	190	90	177	9
Steele et al. (1980)	4.3	2.0	305	60	75	200	6.5
Meyer (1979)		2.6	300				13
Meyer (1979)		1.7	300	91		190	10

TABLE 15415-3. INAA analyses of five plagioclase separates (Palme et al., 1984).

Weight, mg.		42.5	34.5	265	615	816
Na	ppm	2670	2570	4014	4320	4300
Sr	ppm	191	212	246	220	232
Eu	ppb	790	740	1290	1280	1270
Ba	ppm	6	7	21	22	22
La	ppb	140	120	364	391	385
Sm	ppb	38	35	108	103	112
Yb	ppb	<14	<14	32	23	28
Lu	ppb	--	<2	2.4	1.6	2
Fe	ppm	1130	1050	1200	690	852
Sc	ppb	157	155	270	120	216
Cr	ppm	3.6	1	8.5	1.9	3.6
Co	ppb	320	358	88	12	15
Mn	ppm	--	--	40	24	29

CHEMISTRY: Chemical analyses for bulk rock 15415 are listed in Table 4, and the rare earths plotted in Figure 4. The main features of the data are the high alumina and low iron, the high iron/magnesium ratio, the low abundance of rare earths, and the lack of meteoritic siderophile contamination, features remarked upon by various authors. Haskin et al. (1981) analyzed two subsamples for rare earths, finding good agreement except for Lu. They suggested that Lu has anomalous behaviour (not Yb as had been suggested earlier), and also found that La was anomalous among all laboratories. Otherwise the rare earths in 15415 are "appealingly simple." Haskin et al. (1981), Hubbard et al. (1972), and Palme et al. (1984) calculated parental liquids with roughly chondritic rare earth element patterns and abundances ~10x chondrites. A small positive Eu anomaly in some calculations is very sensitive to the distribution coefficient used and may not be real. 15415 has rather primitive rare earth abundances, although its Fe/Mg is higher than many other (mainly Apollo 16) ferroan anorthosites. Palme et al. (1984) performed INAA analysis of five plagioclase separates (Table 3).

15415 is outstandingly low in volatiles and siderophiles (Morgan et al., 1972b). Six of eight volatiles show a constant normalized pattern of $7.2 \pm 0.8 \times 10^{-4}$ x chondrites (Morgan et al., 1976). The data of Reed and Jovanovic (1972) also show low volatiles. The low siderophiles are a standard for demonstrating the presence of meteoritic siderophiles in other samples, e.g., Apollo 11 anorthosites (Morgan et al., 1972a). While the sample contains very little U and Th, the Pb value is disproportionately high (Tatsumoto et al., 1972). Much of the Pb is easily leachable (Tera et al., 1972). The low

Th/U (Tatsumoto et al., 1972; Silver, 1976) reflects the concentration of plagioclase in the absence of large ion lithophile element enrichment.

DesMarais et al. (1973, 1974) provided data on carbon compounds released on combustion, and on H contents. Both total C (see also Moore et al., 1973), and total H abundances are much lower than values for lunar fines. Simoneit et al. (1973) studied the gas release pattern under vacuum with pyrolysis. At low temperatures, H_2O and CO_2 are the absorbed species; at higher temperature low levels of only CO are evolved bimodally. All nitrogen analyses are at background levels.

STABLE ISOTOPES: Oxygen isotopic determinations were made by Epstein and Taylor (1972) who reported δO^{18} (°/oo) of 6.05 ± 0.04, and by Clayton et al. (1972, 1973) and Clayton and Mayeda (1975) who reported δO^{18} (°/oo) for plagioclase of 5.78, 5.71, and 5.84 respectively. These values are similar to other lunar rocks and as expected for igneous processes. Clayton and Mayeda (1975) also reported a δO^{17} (°/oo) of 2.88, hence 15415 lies on the terrestrial/lunar mass fractionation line.

Epstein and Taylor (1972) reported a δSi^{30} (°/oo) of -0.18, similar to other lunar igneous rocks.

Fig. 3a

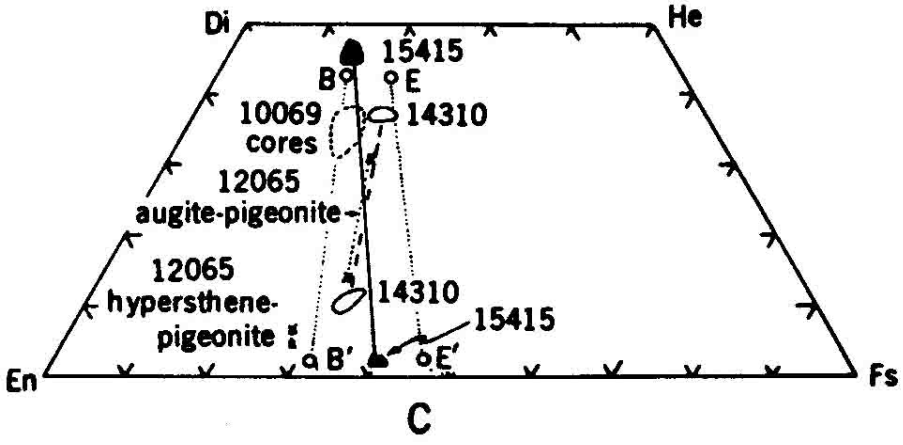

Fig. 3b

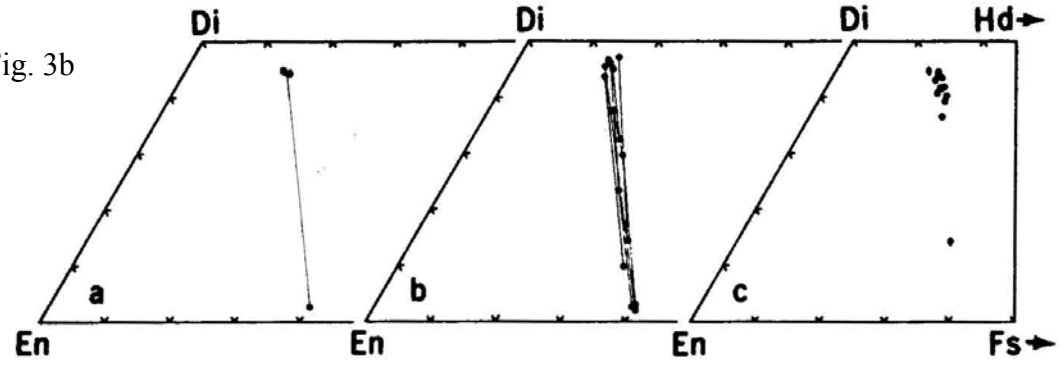

Figure 3. Compositions of pyroxenes in 15415.
a) from Hargraves and Hollister (1972);
b) from James (1972).

TABLE 15415-1. Chemical analyses of bulk samples

		,123	,0	,11	,11	,11	,12(e)	,177	,177			,40 P-1	,40P-2	,40C	,0	,7
Wt %	SiO2	44.08					44.94									
	TiO2	0.02		0.025	0.016		0.02									
	Al2O3	35.49					35.72		35.5							
	FeO	0.23					0.21	0.199	0.202							
	MgO	0.09		0.16			0.53		<0.5							
	CaO	19.68					20.58		21.0							
	Na2O	0.34		0.38	0.38		0.38	0.364	0.356							
	K2O	<0.01	0.012	0.015	0.014	0.015	0.017				0.0151				0.015	
	P2O5	0.01														
(ppm)	Sc						0.40	0.437	0.434							
	V															
	Cr				63		19.0	19.3	20.3							
	Mn	0					42		47							
	Co						0.26	0.194	0.190							
	Ni						3	12.2	13.3							
	Rb			0.17	0.15(a)						0.217					0.19
	Sr	184		178	172		173	202	198		173.3					240.5
	Y															
	Zr															
	Nb															
	Hf						0.017	0.011	0.014							
	Ba			6.2	6.28		6.5	6	6							
	Th		<0.030		0.027					0.0036	0.0034		0.0064	0.0037	0.0035	0.028
	U		0.0024		0.0098	0.0125	0.0015			0.0017	0.0014		0.0034	0.0014	0.00087	<0.005
	Pb									0.268	0.246		0.18	0.28	0.16	
	La				0.118		0.21	0.130	0.133							
	Ce			0.32	0.35			0.320	0.330							
	Pr															
	Nd			0.20	0.175											
	Sm			0.049	0.046		0.062	0.056	0.054							
	Eu			0.807	0.806		0.82	0.805	0.805							
	Gd			0.062	0.050											
	Tb							0.0100	0.0070							
	Dy			0.063	0.044		0.054									
	Ho															
	Er				0.019											
	Tm															
	Yb			0.045	0.035		0.035	0.029	0.028							
	Lu				0.0034		0.0041	0.0036	0.0061							
	Li			1.0	2.0											
	Be															
	B															
	C															
	N															
	S	0														
	F															
	Cl						150									
	Br															
	Cu						57.9									
	Zn						31.8									
(ppb)	I															
	At															
	Ga						3100									
	Ge						20									
	As						4.1									
	Se															
	Mo															
	Tc															
	Ru															
	Rh															
	Pd															
	Ag															
	Cd															
	In															
	Sn															
	Sb															
	Te															
	Cs															
	Ta							31	25							
	W						260									
	Re															
	Os															
	Ir															
	Pt															
	Au						0.77									
	Hg															
	Tl															
	Bi															
		(1)	(2)	(3)	(4)	(5)	(6)	(7)	(7)	(8)	(8)	(8)	(9)	(9)	(9)	(10)	(11)

TABLE 15415-4 Continued

	,?	,42	,42	,12	,45	,44	,9	,9	,7	,7
SiO2										
TiO2										
Al2O3										
FeO										
MgO										
CaO								19.6		
Na2O										
K2O							0.013		0.016	0.014
P2O5										
Sc										
V										
Cr										
Mn										
Co										
Ni										
Rb	0.16			0.11						
Sr	173.4									
Y										
Zr										
Nd										
Hf										
Ba										
Th										
U		0.0066	0.031							
Pb										
La										
Ce										
Pr										
Nd										
Sm										
Eu										
Gd										
Tb										
Dy										
Ho										
Er										
Tm										
Yb										
Lu										
Li		15								
Be										
B										
C					15	3				
N										
S										
F		<0.7								
Cl		0.50(b)								
Br		0.057(b)	0.097(b)	2.3						
Cu										
Zn				0.26						
I		1.1(c)								
At										
Ga										
Ge				1.2						
As										
Se				0.23						
Mo										
Tc										
Ru			<0.5							
Rh										
Pd										
Ag				1.73						
Cd				0.57						
In				0.178						
Sn										
Sb				0.067						
Te		68		2.1						
Cs				23						
Ta										
W										
Re				0.00084						
Os			3.5							
Ir				<0.010						
Pt										
Au				0.117(d)						
Hg										
Tl				0.09						
Bi				0.097						
	(11)	(12)	(12)	(13)	(14)	(15)	(16)	(17)	(18)	(18)

References to Table 15415-4

References and methods:

(1) LSPET (1972); XRF
(2) LSPET (1972); gamma ray spectroscopy
(3) Wiesmann and Hubbard (1975), Nyquist et al. (1972a,b); isotope dilution, mass spec
(4) Wiesmann and Hubbard (1975), Hubbard et al. (1971), Nyquist et al. (1972b); isotope dilution, mass spec
(5) Church et al. (1972); isotope dilution, mass spec
(6) Wanke et al. (1975); XRF, INAA, RNAA
(7) Haskin et al. (1981); INAA
(8) Tatsumoto et al. (1972); isotope dilution, mass spec
(9) Tera et al. (1972); isotope dilution, mass spec
(10) Keith et al. (1972); gamma ray spectroscopy
(11) Wasserburg and Papanastassiou (1971); isotope dilution, mass spec
(12) Reed and Jovanovic (1972), Jovanovic and Reed (1977); Activation (neutron and photon)
(13) Morgan et al. (1972a,b), Ganapathy et al. (1973); RNAA
(14) Moore et al. (1973); combustion, gas chromatography
(15) Desmarais et al. (1973); combustion, gas chromatography
(16) Husain et al. (1972); from Ar isotopes
(17) Husain (1974); from Ar isotopes
(18) Turner (1972); from Ar isotopes

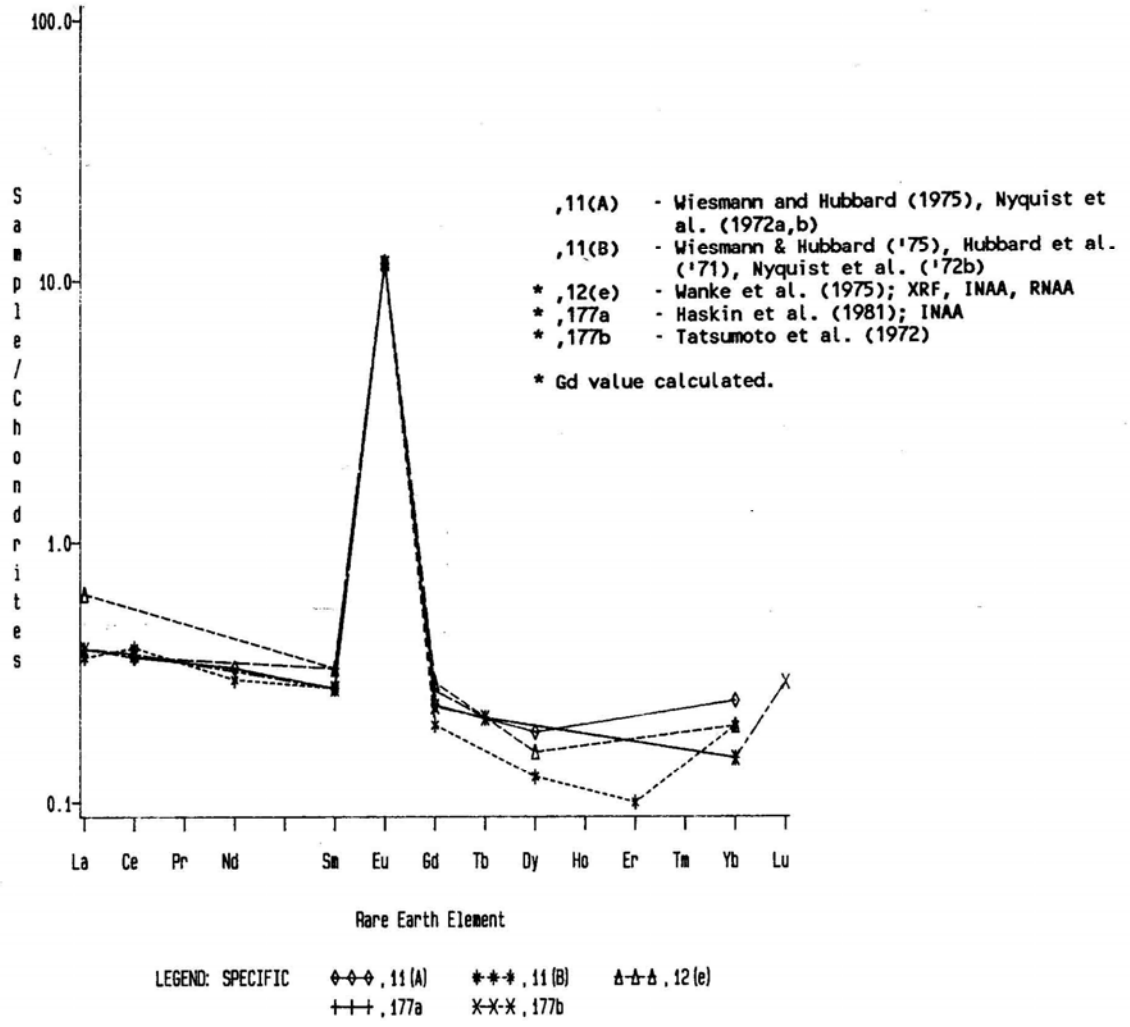

Figure 4. Rare earths in 15415.

RADIOGENIC ISOTOPES AND GEOCHRONOLOGY: ^{40}Ar-^{39}Ar studies by Husain (1972) and Husain et al. (1972a,b), and Turner (1972) give ages of 4.09 ± 0.19 b.y. and 4.05 ± 0.15 b.y. As stated by Turner (1972), there is no evidence of a real plateau, and the age is an "asymptotic high temperature" age, giving a lower limit of 3.9 b.y. to the crystallization age. Husain et al. (1972a) interpreted the age to mean that 15415 was a fragment of 4.1 b.y. old crust, virtually unaffected by post-crystallization thermal effects. However, the sample is probably much older. The sample is retentive, with most radiogenic ^{39}Ar released above 900°C. The Ar losses over the last 4.0 b.y. are 13% (Turner, 1972) or 4% (Husain, 1972a,b). K/Ca is constant with temperature, consistent with release of Ar from a monomineralic rock.

Whole rock Rb-Sr data were provided by Wasserburg and Papanastassiou (1971) and Papanastassiou and Wasserburg (1973), by Nyquist et al. (1972a,b; 1973) and Wiesmann and Hubbard (1975) and by Tatsumoto et al. (1972) (Table 5). These data establish I_o to be less than or equal to BABI. It is clear that 15415 has extremely low Rb/Sr and in the last 4.6 b.y. has never been exposed to an environment with Rb/Sr as high as even the low values observed in low K Apollo 11 mare basalts (Wasserburg and Papanastassiou, 1971). Material forming the rock must have separated from a reservoir with Rb/Sr = 0.0035 (e.g., Apollo 11 rocks) within 3.5 x $l0^8$ years of the formation of the Moon, but no precise statement of age is possible. However, the data demonstrate a maximum formation interval for the Moon of 3 m.y. after the solar system (Rb/Sr = 0.6) had the composition of BABI close to 4.6 b.y. ago (Wasserburg and Papanastassiou, 1971).

U, Th-Pb isotopic data were presented by Tera et al. (1972), and by Tatsumoto et al. (1972) and Nunes et al. (1973). According to Tera et al. (1972) the bulk of the Pb is easily leachable, and is very heterogeneous isotopically. A highly radiogenic Pb is the one easily leached, leaving a residue of primordial Pb; the radiogenic Pb was added post-crystallization. There is no direct evidence for an ancient crust; rather the Pb represents 4.0 b.y. old material. Nunes et al. (1973) noted the complexities in interpretation of ages from the Pb data; if there are components other than in situ radiogenic Pb and modern (terrestrial) Pb, then a simplistic U-Pb age interpretation is not strictly valid.

RARE GASES AND EXPOSURE: Husain et al. (1972a,b) and Husain (1974) reported a ^{38}Ar exposure age of 90 ± 10 m.y., and Turner (1972) a ^{38}Ar exposure age of 112 m.y. While these are similar to a ^{81}Kr-Kr exposure age of 104 ± 15 m.y. by Eugster et al. (1984), the latter found that 15415 had experienced a multistage exposure. They reported detailed analyses for rare gas isotopes. Their investigation was hampered by strongly diffusive losses from their sample, e.g., 98% ^3He_c missing, 40% of radiogenic ^{40}Ar missing, so that the abundances of cosmogenic components do not appear to be reliable. The shielding depth at collection for their subsplit was about 10g/cm^2.

Keith et al. (1972) and Keith and Clark (1974) reported disintegration count data for cosmogenic nuclides. The lack of Fe in the sample led to very low activities for ^{54}Mn, ^{56}Co, and ^{22}Na. The ^{26}Al is unsaturated (Keith and Clark, 1974; Yokoyama et al., 1974) indicating rapid erosion and an exposure of 1.61 (+0.51, -0.34) m.y. based on a one-step elevation to the surface, and representing only the most recent surface residence time.

TABLE 15415-5. Rb-Sr isotopic data for whole-rock 15415

Reference		Rb	Sr	$^{87}Rb/^{86}Sr$	$^{87}Sr/^{86}Sr$	$I_{4.6\ b.y.}$	$I_{4.6\ b.y.}$ (a)
Wasserburg and Papanastassiou (1971)	15415-A	0.196	240	0.0024	0.69926±12	0.69910±12	—
Wasserburg and papanastassiou (1971)	15415-B(b)	0.145	173	0.0027	0.69914±5	0.69898±5	—
Nyquist et al. (1972a,b; 1973)	15415,1	0.17	177	0.0028	0.69938±18	0.69920±18	0.69908±18
Nyquist et al. (1972a,b; 1973)	15415,11	0.142	172	0.0024	0.69926±5	0.69910±5	0.69898±5
Tatsumoto et al. (1972)	15415	0.217	173.3		0.69914		

(a) corrected for interlaboratory bias to C.I.T. data.
(b) preferred value, more precise and larger sample.

PHYSICAL PROPERTIES: Gose et al. (1972) and Pearce et al. (1972, 1973) studied the magnetic properties of 15415. As received the sample was weakly magnetic, with a NRM intensity about 1 x 10^{-6} emu/g, which is two orders of magnitude less than breccias. Alternating field demagnetization is very weak and difficult to measure (sample only 2 g). There seems to be a stable component of about 2 x 10^{-7} emu/g (Fig. 5), extremely weak by comparison with mare basalts and breccias, presumably because there is so little iron. There is no systematic change in direction; the scatter in Figure 5 probably results from the intensity being so close to the detection limit rather than from instability.

Seismic velocities were measured by Chung (1973) and by Mizutani and Newbigging (1973) (Table 6). The data agree well except at low pressure, and the differences presumably result from varied fracturing of the sub-samples. The velocities are less than for terrestrial anorthosites because of the numerous fractures and microcracks in 15415.

TABLE 15415-6. Elastic wave velocities (km/sec)

Pressure Kb	0	0.5	1.0	1.5	2	3	4	5	6	7	9	(10)*	Reference
S	—	2.0	2.5	2.90	3.26	3.42	3.54	3.56	3.58	3.61	—	3.69	Chung, 1973
P	—	5.0	5.6	6.02	6.40	6.65	6.70	6.78	6.83	6.85	—	6.87	Chung, 1973
P	5.98	6.20	6.28	—	6.43	6.56	—	6.75	—	6.89	7.01	—	Mizutani and Newbigging, 1973

Chung and Westphal (1973)reported dielectric spectra data. The high frequency dielectric constant (K') is 4, which is low, and the high frequency dissipation factor (tan δ) is about 0.001, also low.

Hoyt et al (1972)reported on thermoluminescence studies of 15415, giving glow curves (photons detected vs. temperature). The thermoluminescence sensitivity is extremely low, and the glow curve stage is very different from those of fines. Materials such as 15415 can contribute very little to the thermoluminescence of lunar fines.

Spectral reflectance data were reported by Adams and McCord (1972) and Charette and Adams (1977). Both spectra are dominated by the Fe^{2+} plagioclase band at 1.3 microns, but whereas Adams and McCord (1972) found no pyroxene band structure, Charette and

Adams (1977) found a two-pyroxene composite band, and a feature near 0.6 microns that could result from very thin plates of ilmenite in the pyroxene.

PROCESSING AND SUBDIVISIONS: 15415 has been substantially subdivided and widely allocated. Apart from small loose chips, 15415 was originally subdivided by prying off one end (,34) and sawing off another (,33) (Fig. 6). ,33 was entirely subdivided by further sawing to produce the main chips shown in Figure 6. Most allocations were made from the subdivisions of ,33; ,34 was also allocated. In 1975, 30% of ,0 was allocated for remote storage, so it was sawn, with resulting subdivisions shown in Figure 7. ,139 (26.9 g) and ,140 (28.6 g) are stored at Brooks. ,143 now has a mass of 89.7 g and is the largest intact piece of 15415. Ten thin sections were made from each of chip ,3 and from ,55, and one from ,46. Other principal investigator-made thin sections, grain mounts, and TEM foils exist.

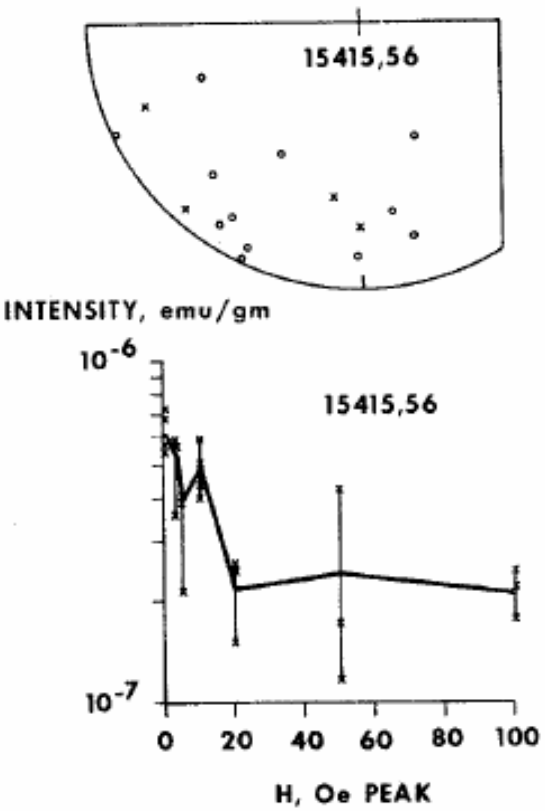

AF demagnetization of anorthosite sample 15415,56. No systematic changes in direction were observed. Error bars on intensity curve represents absolute error for repeat measurements. (The same definition applies to all similar figures.)

Figure 5. AF demagnetization of 15415,56.

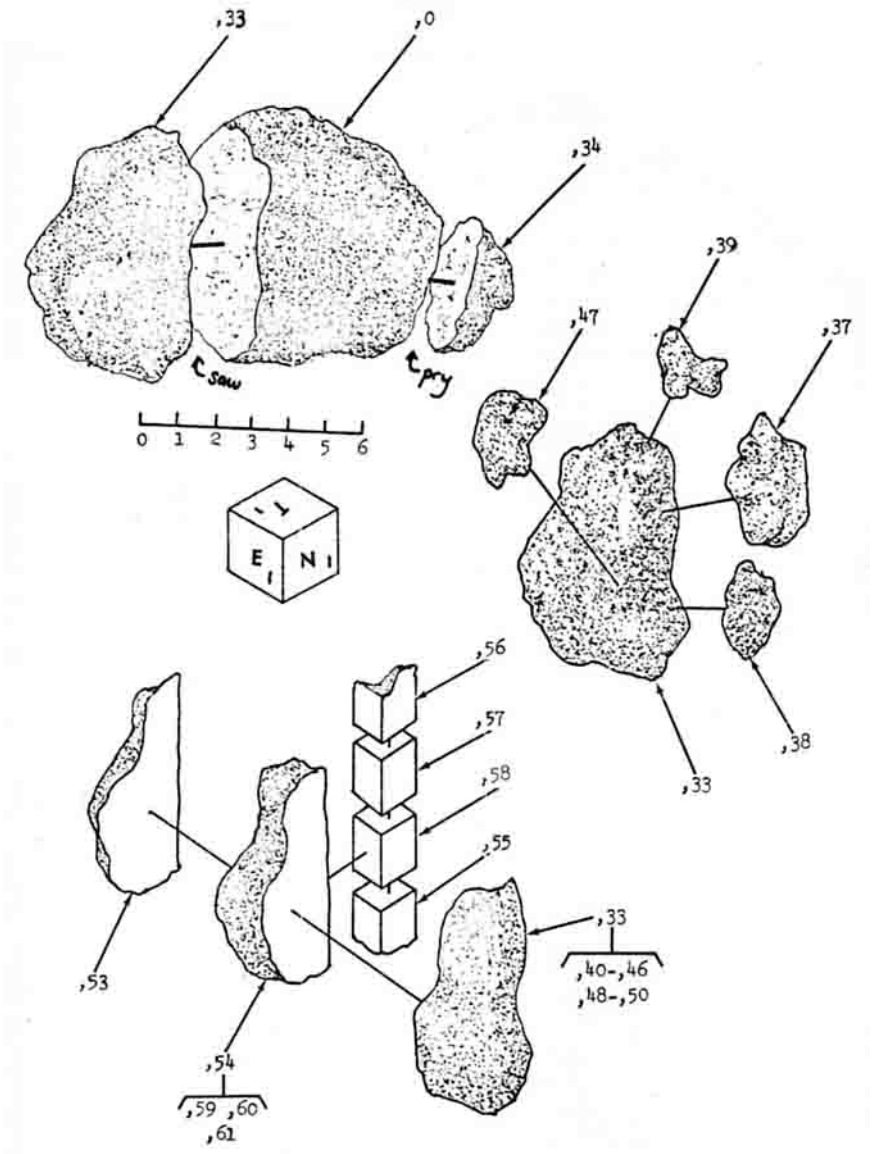

Figure 6. Original subdivision of 15415.

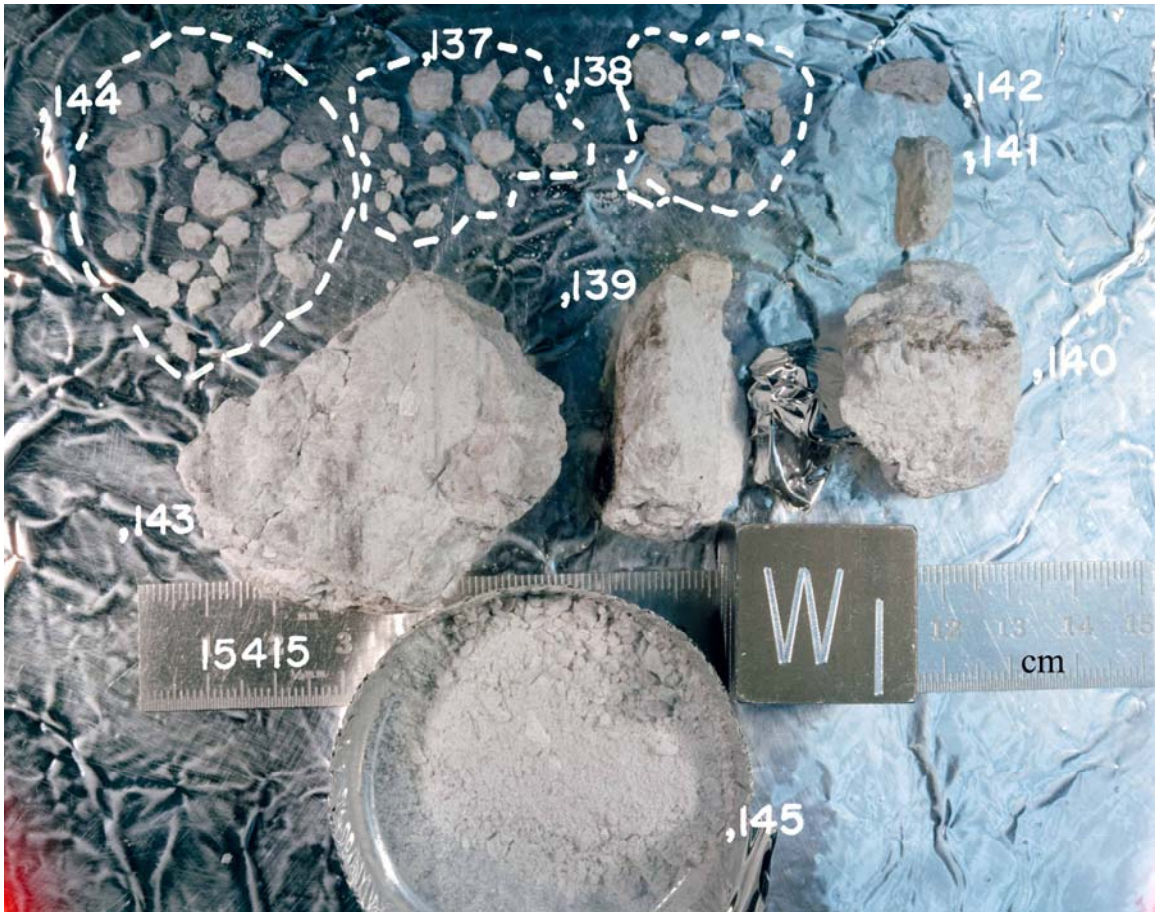

Figure 7. 1975 subdivision of ,0. S-75-32659.